The RopGEF KARAPPO is Essential for the Initiation of Vegetative Reproduction in *Marchantia*

Takuma Hiwatashi,[1] Koh Li Quan,[2] Yukiko Yasui,[1] Hideyuki Takami,[1] Masataka Kajikawa,[3] Hiroyuki Kirita,[3] Mayuko Sato,[4] Mayumi Wakazaki,[4] Katsushi Yamaguchi,[5] Shuji Shigenobu,[5] Hidehiro Fukaki,[1] Tetsuro Mimura,[1] Katsuyuki T. Yamato,[7] Kiminori Toyooka,[4] Shinichiro Sawa,[6] Daisuke Urano,[2] Takayuki Kohchi,[3] and Kimitsune Ishizaki,[1,8*]

[1]Graduate School of Science, Kobe University, Kobe 657-8501, Japan.

[2]Temasek Life Sciences Laboratory, National University of Singapore, Singapore 117604, Singapore.

[3]Graduate School of Biostudies, Kyoto University, Kyoto 606-8502, Japan.

[4]RIKEN Center for Sustainable Resource Science, Yokohama 230-0045, Japan.

[5]Functional Genomics Facility, National Institute for Basic Biology (NIBB), Okazaki, Aichi 444-8585, Japan.

[6]Graduate School of Science and Technology, Kumamoto University, Kumamoto 860-8555, Japan.

[7]Faculty of Biology-Oriented Science and Technology, Kindai University, Kinokawa, Wakayama 649-6493, Japan.

[8]Lead Contact

[*]Corresopondence: kimi@emerald.kobe-u.ac.jp (K.I.)

SUMMARY

Many plants can reproduce vegetatively, producing clonal progeny from vegetative cells; however, little is known about the molecular mechanisms underlying this process. Liverwort (*Marchantia polymorpha*), a basal land plant, propagates asexually via gemmae, which are clonal plantlets formed in gemma cups on the dorsal side of the vegetative thallus [1]. The initial stage of gemma development involves elongation and asymmetric divisions of a specific type of epidermal cell, called a gemma initial, which forms on the floor of the gemma cup [2, 3]. To investigate the regulatory mechanism underlying gemma development, we focused on two allelic mutants in which no gemma initial formed; these mutants were named *karappo*, meaning "empty". We used whole-genome sequencing of both mutants, and molecular genetic analyses to identify the causal gene, *KARAPPO* (*KAR*), which encodes a Rop guanine nucleotide exchange factor (RopGEF) carrying a PRONE catalytic domain. *In vitro* GEF assays showed that the full-length KAR protein and the PRONE domain have significant GEF activity toward MpRop, the only Rop GTPase in *M. polymorpha*. Moreover, genetic complementation experiments showed a significant role for the N- and C-terminal variable regions in gemma development. Our investigation demonstrated an essential role for KAR/RopGEF in the initiation of plantlet development from a differentiated cell, which may involve cell polarity formation and subsequent asymmetric cell division via activation of Rop signaling, implying a similar developmental mechanism in vegetative reproduction of various land plants.

KEYWORDS

asexual reproduction, small GTPase, cell polarity, evolution

RESULTS AND DISCUSSION

Gemma development in *Marchantia polymorpha*

Vegetative reproduction is a form of asexual reproduction in which clonal individuals develop directly from vegetative tissues, such as leaves, stems, and roots. Vegetative reproduction is a developmental process based on totipotency, which is the potential for a cell, even a differentiated cell, to regenerate organs or whole plantlets [4-6]. Many plants in diverse lineages exhibit vegetative reproduction, *e.g*. potato (*Solanum tuberosum*), which produces tubers in underground stems, *Kalanchoe diagremontiana*, which forms plantlets at the leaf margins, the Dhalia family, which develop root tubers, and the hen and chicken fern (*Asplennium bulbiferum*), which grows small bulbils on the top of fronds [7]. However, very little is known about the underlying molecular mechanisms of vegetative reproduction.

One of the most basal lineages in extant land plants, the liverwort *Marchantia polymorpha*, has the ability to propagate asexually by forming clonal plantlets, called gemmae, in a cupule or "gemma cup", a cup-like receptacle formed on the dorsal side of the thallus, which is the gametophyte plant body (Figure S1A). The development of the gemma and gemma cup in *M. polymorpha* has been described on the basis of histological observations [2, 8]. In the basal floor of the gemma cup, epidermal cells undergo cell elongation followed by two cycles of asymmetrical cell division to form an apical gemma cell and a basal cell (Figure S1E). The gemma cell continues to divide and finally produces the discoid gemma with two laterally developed apical notches. The basal cell does not divide any further and differentiates into a stalk cell [1, 2]. Mucilage papillae also develop from individual epidermal cells located in the floor of gemma cups [2, 3]. In our histological observations, various stages of developing gemmae and single-celled mucilage

papillae (large club-shaped cells) were observed in the basal floor of the gemma cup (Figure S1B–D). The elongated morphology of mucilage papillae was distinct, with a number of single-membrane vesicles in their cytosol (Figure S1C). At the initial stage of gemma development, the basal stalk cell was already vacuolated, and the apical gemma cell underwent several rounds of periclinal cell divisions. In most cases, an anticlinal cell division was observed in the basal floor cell attached to the early stage of the developing gemma, while there was no cell division observed in the basal floor cell attached to the mucilage cell (Figure S1B–E).

Isolation of *karappo-1* and *karappo-2* mutants

In recent years, *M. polymorpha* has been exploited as a basal plant model system due to the availability of whole-genome sequence information, high-efficiency transformation methods, and genetic modification techniques [9-16].

To identify key regulator(s) involved in the initial stage of gemma development in *M. polymorpha*, we focused on two mutants, named *karappo-1* (*kar-1*) and *karappo-2* (*kar-2*), that show a common phenotype of impaired gemma formation. These two mutants were isolated independently; *kar-1* was isolated during the screening of T-DNA-tagged lines for morphological phenotypes of the gametophyte thallus [17], and *kar-2* was isolated from transgenic lines generated by biolistic delivery of a plasmid [18]. In the wild type as well as in *kar-1* and *kar-2* mutants, gemma cups formed at intervals on the dorsal side of thalli along the midrib (Figure 1A, B, and C). Numerous mature gemmae were observed from the top of the wild-type gemma cup; however, no gemmae were found in the *kar-1* and *kar-2* mutants (Figure 1F, G, and H). Transverse sections of the gemma cup showed no developing gemmae in the gemma-cup of the *kar-1* and *kar-2* mutants (Figure 1L, M, Q,

and R), while various stages of developing gemmae were observed in the wild type (Figure 1K and P). In contrast, mucilage papillae were formed from the basal epidermis of the gemma cup in the *kar-1* and *kar-2* mutant as in the wild type (Figure 1U, V, and W). There was no distinct impairment in the other aspects of vegetative development in the *kar-1* and *kar-2* mutants compared to the wild type (*i.e*. growth rate of thalli, air chamber formation, and rhizoid development). These observations suggest that the initial stage of gemma development is defective in *kar-1* and *kar-2* mutants.

Molecular characterization of *kar* mutants

The segregation ratio of the mutant gemma phenotype in an F_1 population generated from a cross between the *kar-1* mutant, which is a female, and the wild-type (WT) male accession Takaragaike-1 (Tak-1) was 102:108 (*kar*:WT). This fit the expected 1:1 ratio as indicated by the chi-squared test ($p<0.01$), suggesting the involvement of a single genetic locus in the *kar* phenotype. However, the *kar* phenotype in F_1 progenies segregated independently from the hygromycin-resistant marker in the transformed T-DNA fragment, indicating that the *kar-1* mutation is independent of the T-DNA insertion. The *kar-2* mutant, which is a male line, was infertile in several attempts at crossing with the wild-type female accession Takaragaike-2 (Tak-2).

To identify the causal gene of the *kar-1* and *kar-2* mutant phenotype, we sequenced the whole genomes of these mutants by next-generation DNA sequencing, and mapped the obtained reads on the reference genome of *M*. *polymorpha* [9]. Compared to the wild type, the *kar-1* mutant carried a 9-bp deletion and an 18-bp insertion at the junction of the 5th exon and 5th intron of *Mapoly0171s0028* [9]. As a result, the cDNA sequence of *Mapoly0171s0028* in the *kar1* mutant showed an 11-bp deletion and a 1-bp

121 insertion in the coding sequence, which caused a frame-shift and generated a truncated
122 protein (Figure S2A–C). Furthermore, we identified a deletion of an approximately 20-kb
123 genomic locus containing the entire coding sequence of *Mapoly0171s0028* in the *kar-2*
124 mutant (Figure S2D and E).

125 We then performed genetic complementation tests in the *kar-1* and *kar-2* mutants
126 by introducing the *Mapoly0171s0028* cDNA fragment under the control of its own
127 promoter (*proKAR:KAR*). The resultant transgenic lines in the *kar-1* and *kar-2* mutant
128 backgrounds had restored gemma formation (Figure 1I, J, N, O, S, and T). For further
129 confirmation, we disrupted *Mapoly0171s0028* in the wild type using homologous
130 recombination-mediated gene targeting [11] and isolated two independent knockouts of
131 *Mapoly0171s0028* (Figure 2A and B). The two knockout lines, kar^{KO} #1 and #2, showed a
132 complete loss of gemma formation similar to the *kar* mutants. The impaired gemma
133 formation was recovered by the introduction of citrine-fused wild-type cDNA of
134 *Mapoly0171s0028* (Figure 2C–E). These results indicated that the *kar* phenotype was
135 caused by a loss of function of *Mapoly0171s0028*. This gene was designated as *KARAPPO*
136 (*KAR*) after a Japanese word meaning “empty”, representing the characteristic phenotype
137 of the mutants with empty gemma cups.
138
139 **_KAR_ encodes a potential activator of Rop GTPase signaling**
140 The deduced amino acid sequence of KAR encodes a highly conserved plant-specific Rop
141 nucleotide exchanger (PRONE) catalytic domain, which is characteristic of the guanine
142 nucleotide exchange factor (GEF) of the Rop GTPase [19], while the N- and C-terminal
143 regions outside of the PRONE domain were highly variable (Figure S3). In angiosperms,
144 Rop signaling mediated by RopGEF is involved in various developmental processes and

145 environmental responses [20-25]. *KAR* is the sole PRONE-type RopGEF gene in the *M*.
146 *polymorpha* genome. In addition, the *M*. *polymorpha* genome also contains only a single
147 copy of *Rop*, *Mapoly0051s0092*, designated as Mp*Rop*, which showed a high overall
148 similarity to *Rop* in various plant lineages (Figure S4A and C).

149 To determine whether *KAR* encodes a functional GEF that acts on MpRop, we
150 examined the interaction of KAR and MpRop by a yeast two-hybrid assay. Yeast cells
151 co-transformed with a combination of either AD::KAR and BD::MpRop or AD::MpRop
152 and BD::KAR grew on selective –W/L/H and –W/L/H/A medium (Figure 3A), indicating
153 that KAR and MpRop physically interact. The interaction between KAR and MpRop was
154 further confirmed by an *in vitro* pull-down assay. The predicted protein coding sequence of
155 KAR was fused to the C-terminus of the 6x Histidine-tag. Purified 6xHis-KAR fusion
156 proteins were pulled down with guanosine triphosphate (GTP)-bound, guanosine
157 diphosphate (GDP)-bound, or nucleotide-free forms of the glutathione S-transferase
158 (GST)-MpRop fusion protein and were detected using anti-His antibody. KAR fusion
159 proteins exhibited similar interactions with different forms of MpRop *in vitro* (Figure 3B).

160 Next, we examined the GEF activity of KAR toward MpRop (Figure 3C). In
161 *Arabidopsis thaliana*, there are 14 RopGEFs with a high degree of sequence similarity to
162 the residues that are involved in catalyzing GDP/GTP exchange [26]. In Arabidopsis, the
163 PRONE domain is sufficient for catalysis of nucleotide exchange on ROP [19] [26], while
164 the variable C-terminal domain of some RopGEFs autoinhibits GEF activity [26]. To test
165 the GEF activity and the potential regulatory role in the variable regions of KAR, we
166 purified the full-length KAR protein and a truncated version of KAR containing just the
167 PRONE domain (KAR-PRONE), and characterized their GEF activity toward MpRop
168 using radio-labelled [^{35}S]-GTPγS. We detected significant GEF activities toward MpRop

with full-length KAR and KAR-PRONE, and the GEF activity of full-length KAR was comparable to that of KAR-PRONE (Figure 3C).

We tested the functionality of the *KAR-PRONE* coding sequence without the N- and C- terminal region in gemma formation. Two lines with comparable expression levels of the full-length *KAR* or the *KAR-PRONE* coding sequence were selected for further analysis (Figure 3D). Introduction of citrine-fused full-length *KAR* cDNA restored to some extent the formation of gemma with normal morphology in the kar^{KO} #2 background. By contrast, the citrine-fused KAR-PRONE did not lead to the full recovery of gemma formation; the most of the gemmae were abnormal in size and morphology with an irregular periphery (Figure 3E). These results demonstrated that the N-terminal and C-terminal variable regions of KAR play a significant role in proper gemma formation *in vivo*, although they have no obvious effect on GEF activity in vitro (Figure 3C).

Ubiquitous expression of *KAR* and Mp*Rop* in vegetative tissues

To evaluate the expression pattern of *KAR* and Mp*Rop*, we generated transgenic *M. polymorpha* lines expressing the β-glucuronidase (*GUS*) reporter gene under the control of the *KAR* promoter (*proKAR:GUS*) and the Mp*Rop* promoter (*pro*Mp*Rop:GUS*). In *proKAR:GUS* and *pro*Mp*Rop:GUS* lines, GUS staining was observed in the broader region of the entire thallus, including the basal floor of the gemma cups containing developing gemmae (Figure 4A and B). We further evaluated the expression pattern of *KAR* and Mp*Rop* using reverse-transcription quantitative PCR (RT-qPCR). Transcripts of *KAR* and Mp*Rop* were detected in all stages and organs in the vegetative thallus (Figure 4C). These results suggest that *KAR* and Mp*Rop* are ubiquitously and simultaneously expressed in the initial stage of gemma development.

193 Knockout plants of Mp*Rop* were generated by homologous
194 recombination-mediated gene targeting; however, two independent Mp*Rop*^{KO} lines showed
195 severe impairment of thallus growth and wilted before the formation of the gemma cup
196 (Figure S4B). This result suggests a much broader function for the sole Rop in *M*.
197 *polymorpha*, which is evidently essential for the growth and development of the
198 gametophyte thallus. Another type of GEF, SPIKE1 (SPK1), has been reported to regulate
199 cytoskeletal rearrangement and cell-shape change in response to growth signals in
200 angiosperms [27, 28]. SPK1 has a conserved DOCK homology region 2 (DHR2) domain,
201 which is distantly related to CZH [CDM (Ced-5, Dock180, Myoblastcity)-Zizimin
202 homology] RhoGEFs in animals and fungi [29]. *M*. *polymorpha* contains a single *SPK1*
203 homologue, Mp*SPK1* [9] (Figure S4C), which may have a critical function in controlling
204 Rop signaling in thallus growth.

205 The contrast between the specific developmental impairment in *kar* mutant lines
206 (Figure 1 and 2), and the ubiquitous promoter activity of *KAR* and Mp*Rop* (Figure 4),
207 suggests an upstream regulatory mechanism for KAR activity, which enables cell-type
208 specific activation of Rop in the gemma initial. Recent studies have shown that several
209 plasma membrane-localized receptor-like protein kinases (RLKs) function as upstream
210 regulators of Rop signaling through interaction with the C-terminal variable region of
211 RopGEF (*i*.*e*. the pollen receptor kinases in tomato (*Solanum lycopersicum*) and FERONIA
212 in *Arabidopsis thaliana*) [20, 21, 30]. Similar to their role in polarized cell growth mediated
213 by Rop signaling in angiosperms, RLK(s) might be involved in the specific function of
214 KAR in the initial stage of gemma development in *M*. *polymorpha*. Further functional
215 studies on the N-terminal and C-terminal variable regions of KAR will be needed to
216 understand the regulatory mechanism of Rop signaling in *M*. *polymorpha*.

Role of KAR in the initial stage of gemma development

In this study, we demonstrated that *KAR*, which encodes a RopGEF, is an essential factor required for the initial stage of gemma development in *M. polymorpha*. Histological studies have suggested the occurrence of cell protrusion and subsequent asymmetric cell divisions in the initial stage of gemma development in the epidermal floor of the gemma cup (Figure S1; [2]). A recent study in *M. polymorpha* demonstrated that a ROOT-HAIR DEFECTIVE SIX-LIKE (RSL) class I basic helix-loop-helix (bHLH) transcription factor, MpRSL1, controls the morphogenesis of structures derived from individual epidermal cells (*i.e.* rhizoids, slime papillae, mucilage papillae, and gemmae) [3]. Similar to the loss-of-function mutants of Mp*RSL1*, in the *kar* mutants, we did not observe the one- or two-cell stage of gemma development. On the other hand, the other epidermis-derived structures, mucilage papillae and rhizoids, were generated normally in the *kar* mutants, but are absent in Mp*rsl1* mutants [3]. Mucilage papillae and rhizoids do not undergo any further cell division after polarized cell growth, whereas the development of gemmae involves subsequent asymmetrical cell division and further cell divisions. These observations suggest that KAR promotes the asymmetrical cell division(s) of the gemma precursor cell after the specification of an epidermal cell controlled by MpRSL1.

KAR contains a highly conserved PRONE domain (Figure S3), which has been implicated in the activity of the GEF of Rop GTPase [19, 26]. In this study, we demonstrated the GEF activity of KAR on MpRop *in vitro* (Figure 3). The *Arabidopsis thaliana* genome contains 14 RopGEFs, and Rop signaling mediated by RopGEF is involved in the control of polar cell growth of pollen tubes and root hairs [20-23]. This polar growth involves the coordination of cytoskeleton organization and vesicular

241 trafficking [31, 32]. In yeast and animals, the closest homologues of Rop, the Cdc42 Rho
242 GTPases, regulate polarity and play a key role in the control of asymmetrical cell division
243 [33, 34]. Recently in monocots, Rop was shown to be involved in the asymmetrical
244 division of the stomata mother cell by controlling cytoskeletal scaffolds and nuclear
245 positioning [35, 36]. KAR-mediated Rop signaling could function in the formation of cell
246 polarity and/or subsequent asymmetrical cell divisions during the initiation of gemma
247 development.

248 Vegetative reproduction can be considered as a type of naturally occurring somatic
249 embryogenesis, in which a meristem is regenerated from differentiated cells. In the
250 development of somatic embryos from single cells isolated from tissue cultures of carrot
251 (*Daucus carota* subsp. *sativus*), the first cell division occurs asymmetrically, and one of the
252 daughter cells gives rise to a three-dimensional cell mass from which one or more embryos
253 develop [4-6]. Asymmetrical cell division to produce daughter cells of a different cell fate
254 must be a common key process in the initial stage of organ/plantlet regeneration from
255 differentiated cells. RopGEF-mediated Rop signaling seems to have been acquired in the
256 common ancestor of land plants after the emergence of charophycean algae. PRONE-type
257 RopGEFs have highly diverged in the course of land plant evolution, while the basal land
258 plant *M. polymorpha* has a limited gene repertoire for Rop signaling (Figure S3 and S4).
259 The Rop-driven asymmetric cell division of differentiated cells to regenerate clonal
260 progenies could be a key innovation for sessile land plants to dominate the terrestrial
261 ecosystem, and this mechanism may have been co-opted to regulate numerous
262 physiological and developmental processes, probably also including vegetative
263 reproduction or organ regeneration, in the course of land plant evolution.
264

CONTACT FOR REAGENT AND RESOURCE SHARING

Further information and requests for resources and reagents should be directed to and will be fulfilled by the Lead Contact, Kimitsune Ishizaki (kimi@emerald.kobe-u.ac.jp). Please note that the transfer of transgenic plants will be governed by an MTA, and will be dependent on appropriate import permits being acquired by the receiver.

SUPPLEMENTAL INFORMATION

Figures S1–S4, and Table S1.

AUTHOR CONTRIBUTIONS

T.H. and K.I. designed the research, and T.H. performed most of the experiments. K.I. isolated the *kar-1* mutant and H.K. performed linkage analyses. M.K. and K.T.Y. isolated *kar-2* mutants. T.H., Y.Y., and H.T. performed the histology. K.L.Q. and D.U. performed the *in vitro* pull-down and GEF assays. K.I., K.Y., S.Sh., S.Sa., and T.K. performed the whole-genome sequencing. M.S., M.W., and K.T. performed TEM analyses. T.H., K.I., and T.K. performed the gene-targeting experiments. T.H., K.I., Y.Y., D.U., H.F., and T.M. analyzed the data. T.H., Y.Y., and K.I. wrote the article.

ACKNOWLEDGMENTS

The authors thank Shohei Yamaoka and Ryuichi Nishihama for critically reading the manuscript; Tatsuaki Goh, Kohichi Toyokura, and Miwa Ohnishi for discussions; Sakiko Ishida, Yoriko Matsuda, and Chiho Hirata for technical assistance. Whole-genome sequencing was supported by NIBB Collaborative Research Programs (15-823 to K.I.). This study was supported by MEXT KAKENHI Grants-in-Aid for Scientific Research on Innovative Area (25113009 to T.K., and 25119711, 25114510, and 17H06472 to K.I.), JSPS KAKENHI Grants-in-Aid for Scientific Research (B) (15H04391 to K.I.), and by the Asahi Glass Foundation and SUNTORY Foundation for Life Sciences (to K.I.).

FIGURE LEGENDS

Figure 1. Phenotype of the *kar* mutants and their complimented lines

(A–Y) Five genotypes are presented, one in each column: (first column) wild type, (second column) *kar-1*, (third column) *kar-2*, (fourth column) *kar-1* complementation line (*kar-1* transformed with *proKAR:KAR*), (fifth column) *kar-2* complementation line (*kar-2* transformed with *proKAR:KAR*). **(A–E)** Top view of 2-week-old thalli grown from tips of thalli. Scale bars represent 1 mm. **(F–J)** Surface view of gemma cups in 2-week-old thalli. Scale bars represent 1 mm. **(K–O)** Toluidine-blue-stained transverse sections of gemma cups in 2-week-old plants. Scale bars represent 100 µm. **(P–Y)** Magnified views of toluidine-blue-stained sections of gemma cups in 2-week-old plants. Arrowheads and arrows indicate gemma initials and mucilage papillae, respectively. Scale bars represent 10 µm.

Figure 2. Generation of knockout mutants of *KAR*

(A) Schematic representation of the structure of the wild-type *KAR* locus (top), the construct designed for gene targeting (middle), and the *KAR* locus disrupted in the gene-targeted lines (bottom). Each primer pair used for genotyping is indicated by arrowheads and marked with (F) for forward or (R) for reverse. Open boxes indicate exons. **(B)** Genomic PCR analysis of the KAR^{KO} lines using the primers indicated in (A). **(C, D)** Scanning electron microscopy of gemma cups in three genotypes are presented: kar^{KO}*#1* **(C)**, and a representative kar^{KO} line transformed with *proKAR:C-KAR*, which contains a citrine-fused *KAR* coding sequence under the endogenous *KAR* promoter. **(D)**. Scale bars represent 100 µm. **(E)** Number of gemmae formed in a gemma cup in 3-week-old thalli grown from apical fragments in the wild type, a kar^{KO} line, and a representative kar^{KO} complemented line (Values are means ± SD, n = 5).

Figure 3. KAR has GEF activity towards MpRop.

(A) Yeast two-hybrid experiments. Clones in the pGBKT7 vector containing the Gal4-binding domain (BD) are noted in the left column and clones in the pGADT7 vector containing the Gal4 activation domain (AD) are noted in the right column. Growth with

serial dilutions on the –L, –W dropout media indicates that both pGBKT7 and pGADT7 vectors were present. Growth with serial dilutions on the –L, –W, –H dropout media and –L, –W, –H, –A dropout media indicates a physical interaction between the BD and AD fusion proteins. **(B)** Physical interaction of KAR with MpRop. His6-KAR was pulled down with GST or GST-MpRop1 using glutathione agarose. The pull-down samples were separated on a SDS-PAGE gel, then visualized by western blot with an anti-6xHis antibody. **(C)** GEF activity of the full-length KAR (KAR) or the PRONE domain of KAR (KAR-PRONE) toward MpRop. [^{35}S]-GTPγS binding to 1 μM GST-MpRop1 was analyzed over time at 4°C. Graphs show data from two experiments. Fitting curves were estimated by the one-phase association model in GraphPad Prism software. **(D)** RT-qPCR analysis of *KAR* or *KAR-PRONE* expression in 3-week-old wild type and the respective complementation lines shown in Figure 3E. Mp*APT* was used as a control gene. Data are displayed as means ± SD (n = 3). **(E)** Genetic complementation with the full-length *KAR* and the truncated *KAR* coding sequence containing only the PRONE domain. The histogram shows distribution of the different classes of gemmae in a gemma cup in 3-week-old thalli grown from apical fragments, in WT, a *kar*^{KO} mutant, and two representative *kar* complementation lines with the full-length KAR (*proKAR:C-KAR*) and with the PRONE domain (*proKAR:C-PRONE*) (Values are means ± s.d., n=4~5). Tukey's test was performed for the number of normal gemmae, and letters above the bars indicate significant differences at $p < 0.05$. Right panels show pictures of normal gemma of over 500 μm diameter (normal), abnormal gemma with more than two notches, and small gemma of less than 500 μm diameter.

Figure 4. Expression of KAR and MpRop in vegetative tissues

(A, B) Histological GUS activity staining of representative proKAR:GUS **(A)** and proRop:GUS **(B)** transgenic lines. **(C)** RT-qPCR analysis of *KAR* and Mp*Rop* in 1-week-old thalli yet to develop gemma cups (1w thallus), mature gemmae in gemma cups (gemma), gemma cups containing developing gemmae (gemma cups), and midribs. Total RNA was isolated from the respective tissues of Tak-1. *EF1α* was used as a control gene. Data are displayed as means ± SD (n = 3).

STAR METHODS

KEY RESOURCES TABLE

(Attached)

CONTACT FOR REAGENT AND RESOURCE SHARING

Further information and requests for resources and reagents should be directed to and will be fulfilled by the Lead Contact, Kimitsune Ishizaki (kimi@emerald.kobe-u.ac.jp). Please note that the transfer of transgenic lants will governed by an MTA, and will be dependent on appropriate import permits being acquired by the receiver.

EXPERIMENTAL MODEL AND SUBJECT DETAILS

Plant Materials and Growth Conditions

Female and male accessions of *M. polymorpha*, Takaragaike-2 (Tak-2) and Takaragaike-1 [10], respectively (Ishizaki et al. 2008), were used as the wild type. F_1 spores generated by crossing Tak-2 and Tak-1 plants were used for transformation to generate the *kar-1* mutant and the *kar* knockout lines. Thalli were grown on 1% (w/v) agar medium containing half-strength Gamborg's B5 salts [37] under 50–60 μmol m^{-2} s^{-1} continuous white light with a cold cathode fluorescent lamp (CCFL; OPT-40C-N-L; Optrom, Japan) or white light-emitting diodes (white LED; VGL-1200W; SYNERGYTEC, Japan) at 22°C. For crossing, over 2-week-old thalli were transferred to continuous light conditions with 50–60 μmol m^{-2} s^{-1} white LED and 20–30 μmol m^{-2} s^{-1} far red light-emitting diodes (VBL-TFL600-IR730, Valore, Japan).

METHOD DETAILS

Phenotype Analysis and Histology

Two-week-old thalli developed from tips of thalli were dissected into small pieces and transferred to fixative solution with 2% glutaraldehyde in 0.05 M phosphate buffer (pH 7.0) and evacuated with a water aspirator until the specimens sank, then fixed for 2 days at

384 room temperature. The samples were dehydrated in a graded ethanol series and embedded
385 in Technovit 7100 plastic resin. Semi-thin sections (5-μm thickness) were obtained with a
386 microtome (HM 335E, *Leica* Microsystems) for light microscopy and stained with
387 toluidine blue O. Sections were observed with an upright microscope (Axio Scope. A1,
388 Carl Zeiss Microscopy).
389 Cultured thalli of *M. polymorpha* were observed using a digital microscope (VHX-5000,
390 KEYENCE). For scanning electron microscopy, thalli were frozen in liquid nitrogen and
391 observed with a scanning electron microscope (VHX-D500, KEYENCE).
392
393 **Electron microscopy**
394 Samples were fixed with 4% paraformaldehyde and 2% glutaraldehyde in 50 mM sodium
395 cacodylate buffer (pH 7.4) for 2 h at room temperature and overnight at 4°C, then
396 post-fixed with 1% osmium tetroxide in 50 mM cacodylate buffer for 3 h at room
397 temperature. After dehydration in a graded methanol series (25, 50, 75, 90, and 100%), the
398 samples were embedded in Epon812 resin (TAAB). Ultrathin sections (100 nm) or
399 semi-thin sections (1 μm) were cut by a diamond knife on an ultramicrotome (Leica EM
400 UC7, Leica Microsystems, Germany) and placed on a glass slide. The sections were stained
401 with 0.4% uranyl acetate followed by lead citrate solution and coated with osmium under
402 an osmium coater (HPC-1SW, Vacuum Device, Japan). The coated sections were observed
403 with a field-emission scanning electron microscope SU8220 (Hitachi High technology,
404 Japan) with an yttrium aluminum garnet backscattered electron detector at an accelerating
405 voltage of 5 kV.
406
407 **Genome sequencing of the *kar-1* and *kar-2* mutants**
408 Genomic DNA was extracted from *kar-1*, *kar-2*, and Tak-2 plants as follows: the tissue was
409 powdered in liquid nitrogen and incubated in 10 mL hexadecyltrimethylammonium
410 bromide (CTAB) buffer (1.5% CTAB, 75 mM Tris-HCl [pH 8.0], 15 mM EDTA, and 1 M
411 NaCl) for 20 min at 56°C. This suspension was mixed with an equal volume of
412 chloroform:isoamyl alcohol (24:1, w/v), incubated for 20 min at room temperature, and
413 centrifuged at 4,000 × g for 20 min. The aqueous phase was used to repeat the

414 chloroform:isoamyl alcohol extraction, and then mixed gently with 1.5 volumes of CTAB
415 precipitation buffer (1% CTAB, 50 mM Tris-HCl [pH 8.0], and 10 mM EDTA). After
416 centrifugation at 10,000 × g for 30 min at 20°C, the precipitate was dissolved in 1 M
417 sodium chloride containing 10 mg/mL RNaseA and incubated for 30 min at 37°C. The
418 genomic DNA was precipitated with ethanol, dissolved in TE buffer (10 mM Tris-HCl [pH
419 8.0] and 1 mM EDTA), and further purified using a Genomic-tip 100 column (QIAGEN,
420 Germany). The DNA was then sheared on a Covaris sonicator (Covaris, USA),
421 size-selected with Pippin Prep (Sage Science, USA), and used to create the libraries using
422 the TruSeq DNA Sample Preparation Kit (Illumina) with an insert size of ~350 bp. The
423 libraries were sequenced using Illumina HiSeq 2000 with a 2 × 101-nt paired-end
424 sequencing protocol. The sequence reads were mapped to the *M*. *polymorpha* genome
425 sequence [9] and the plasmid sequence was used for the biolistic transformation [18] by
426 Bowtie2 v.2.2.9 [38] with default parameters, and visualized and assessed using Integrative
427 Genomics Viewer v.2.3.23 [39].
428
429 **Characterization of mutations in *KAR*/*Mapoly0171s0028***
430 Small pieces (3 × 3 mm) of thalli were taken from individual plants and crushed with a
431 micro-pestle in 100 µl buffer containing 100 mM Tris-HCl, 1 M KCl, and 10 mM EDTA
432 (pH 9.5). Sterilized water (400 µl) was added to each tube and a 1 µl aliquot of the extract
433 was used as a template for PCR using KOD FX Neo DNA polymerase (Toyobo). To
434 identify the mutation in the *kar-1* mutant, the *Mapoly0171s0028* locus was amplified by
435 genomic PCR using the primer set kar-1_gF/kar-1_gR and sequenced. The cDNA of *kar* in
436 the *kar-1* mutant was amplified by RT-PCR using the primer set KAR-cds-F/KAR-cds-sR
437 and sequenced. To confirm the absence of *Mapoly0171s0028* in the *kar-2* mutant, genomic
438 PCR was performed with a KOD FX Neo DNA polymerase using primers
439 KAR-gF/KAR-gR. Primer pairs are shown in Figure S2D and Table S1.
440
441 **Complementation tests**
442 For complementation of the *kar* mutants, the coding sequence of full-length *KAR* and the
443 truncated coding sequence of *KAR* (*KAR-PRONE*), containing just the PRONE domain

(residues 132–503) were amplified by RT-PCR using KOD plus neo (TOYOBO) with the primer set KAR-cds-F/KAR-cds-sR and PRONE-L/PRONE-R, respectively. The *KAR* and *KAR-PRONE* coding sequence fragments were cloned into the pENTR/D-TOPO cloning vector (Life Technology) to produce pENTR-KAR and pENTR-PRONE, respectively. The *KAR* promoter region, including about 5 kb upstream of the initiation codon, was amplified from Tak-1 genomic DNA by PCR using KOD-Plus-Neo (TOYOBO) with the primer set KARpro_GW_F/KARpro_GW_302_R. The PCR-amplified product was cloned into the *Xba*I and *Hind*Ⅲ sites of pMpGWB302 to replace the CaMV35S promoter [40] with the In-Fusion HD cloning kit (Clontech, Mountain View, CA). The entry vector containing the *KAR* coding sequence was introduced into the binary vector by Gateway LR clonase II Enzyme mix (Thermo Fisher Scientific, USA) to generate the *proKAR:KAR* construct. The *proKAR:KAR* vector was introduced into regenerating thalli of *kar-1* and *kar-2* mutants via *Agrobacterium tumefaciens* GV2260 [13].

Similarly, the *KAR* promoter region, including about 5 kb upstream of the initiation codon, was amplified from Tak-1 genomic DNA by PCR using KOD-Plus-Neo (TOYOBO) with the primer set KARpro_GW_F/KARpro_GW_305_R. The PCR-amplified product was cloned into the *Xba*I and *Hind*Ⅲ sites of pMpGWB305, which contains citrine gene in front of the gateway cassette, to replace the CaMV35S promoter [40] with the In-Fusion HD cloning kit (Clontech, Mountain View, CA). The coding sequence fragments of *KAR* and *KAR-PRONE* in the entry vectors pENTR-KAR and pENTR-PRONE were introduced into the binary vectors by Gateway LR clonase II Enzyme mix (Thermo Fisher Scientific, USA) to generate the *proKAR:C-KAR*, and *proKAR:C-PRONE* constructs, respectively. The binary vector was transformed into the kar^{KO} line. Transformants were selected with 0.5 μM chlorsulfuron and 100 μg/ml cefotaxime.

Generation of KAR^{KO} and MpRop^{KO} plants

To generate the *KAR*-targeting vector, 5′- and 3′-homologous arms (approximately 4.5-kb in length) were amplified from Tak-1 genomic DNA by PCR using KOD FX Neo (TOYOBO) with the primer pairs shown in Table S1. The PCR-amplified 5′- and 3′-homologous arms were cloned into the *Pac*I and *Asc*I sites, respectively, of pJHY-TMp1

474 [11] with the In-Fusion HD cloning kit (Clontech, Mountain View, CA). The *KAR*-targeting
475 vector was introduced into F_1 sporelings derived from sexual crosses between Tak-1 and
476 Tak-2 via *Agrobacterium tumefaciens* GV2260 [10]. The transformed plants carrying the
477 targeted insertions were selected by genomic PCR with a KOD FX Neo DNA polymerase
478 and primer pairs shown in Figure 2 and Table S1.
479 To generate the Mp*Rop*-targeting vector, 5′- and 3′-homologous arms (approximately
480 4.5-kb in length) were amplified from Tak-1 genomic DNA shown in Table S1. The
481 PCR-amplified 5′- and 3 ′-homologous arms were cloned into the *Pac*I and *Asc*I sites,
482 respectively, of pJHY-TMp1 [11] with the In-Fusion HD cloning kit (Clontech, Mountain
483 View, CA). The Mp*Rop*-targeting vector was transformed into F_1 sporelings derived from
484 sexual crosses between Tak-1 and Tak-2 as described above. The transformed plants
485 carrying the targeted insertions were selected by genomic PCR with a KOD FX Neo DNA
486 polymerase and primer pairs shown in Figure S4B and Table S1.
487
488 **Promoter reporter analyses**
489 The *KAR* genomic sequence, including approximately 5 kb upstream of the initiation codon,
490 was amplified from Tak-1 genomic DNA by PCR using KOD-Plus-Neo (TOYOBO) with
491 the primer set KARpro_F/KARpro_R and was cloned into pENTR/D-TOPO (Thermo
492 Fisher Scientific). Similarly, the Mp*Rop* genomic region, including about 3 kb upstream of
493 the initiation codon, was amplified from Tak-1 genomic DNA by PCR with the primer set
494 MpRoppro_F/MpRoppro_R and was inserted into pENTR/D-TOPO (Thermo Fisher).
495 These entry vectors were introduced into the Gateway binary vector pMpGWB104 [40]
496 using Gateway LR clonase II Enzyme mix (Thermo Fisher Scientific, USA) to generate
497 *proKAR:GUS* and *proMpRop:GUS* binary constructs, respectively. The *proKAR:GUS* and
498 *proMpRop:GUS* vectors were introduced into regenerating thalli of Tak-1 via
499 *Agrobacterium tumefaciens* GV2260 [13]. Transformants were selected with 0.5 μM
500 chlorsulfuron and 100 μg/ml cefotaxime. For histological GUS activity assays,
501 transformants were incubated in GUS staining solution (0.5 mM potassium ferrocyanide,
502 0.5 mM potassium ferricyanide, and 1 mM X-Gluc) at 37°C and later cleared with 70%
503 ethanol (Jefferson et al., 1987).

Yeast Two-Hybrid (Y2H) assay

To construct AD::KAR and AD::MpRop vectors, the *KAR* and Mp*Rop* coding sequences were amplified by PCR using KOD plus neo (TOYOBO) with primer pairs KAR_WT_Y2H_pGADT7_F and KAR_WT_Y2H_pGADT7_R, and Rop_WT_Y2H_pGADT7_F and Rop_WT_Y2H_pGADT7_R, respectively, and subcloned into the *Not*I site of pGADT7-AD in Matchmaker Gold Yeast Two-Hybrid System (Takara Bio, Japan) with the In-Fusion HD cloning kit (Takara Bio). To construct BD::KAR and BD::MpRop vectors, the *KAR* and Mp*Rop* coding sequences were amplified by PCR using KOD plus neo (TOYOBO) with primer pairs KAR_WT_Y2H_pGBKT7_F and KAR_WT_Y2H_pGBKT7_R, and Rop_WT_Y2H_pGBKT7_F and Rop_WT_Y2H_pGBKT7_R, respectively, and subcloned into the NotI site of pGBKT7 in Matchmaker Gold Yeast Two-Hybrid System (Takara Bio) with the In-Fusion HD cloning kit (Takara Bio). Indicated combinations of plasmids were co-transformed into yeast strain Y2H Gold (Takara Bio) following the protocol for high-efficiency transformation of yeast with lithium acetate, single-stranded carrier DNA, and polyethylene glycol. Following transformation, colonies were selected for the presence of the plasmids, inoculated in liquid synthetic drop-out (SD) media (lacking the amino acids leucine and tryptophan, with the exception of untransformed strain Y2H Gold, which was grown in YPD), grown to saturation, and plated onto SD media plates lacking the indicated amino acids. SD media plates lacked the amino acids leucine, tryptophan, and histidine (SD –Leu/–Trp/–His). Serial 1:5 dilutions were made in water and 3 µl of each dilution was used to yield one spot. Plates were incubated at 30°C for two (SD –Leu/–Trp) or three (SD –Leu/–Trp/–His) days before taking pictures.

Protein purification

The cDNA of MpRop was amplified by RT-PCR using KOD plus neo (TOYOBO) with primer pairs MpRop-cds-F and MpRop-cds-sR and cloned into pENTR/D-TOPO (Thermo Fisher Scientific). The Mp*Rop* coding sequence in the resultant ENTRY clone and pENTR-KAR and pENTR-PRONE generated above were transferred using Gateway LR

clonase II Enzyme mix (Thermo Fisher Scientific, USA) into the bacterial expression vectors pDEST15 or pDEST17, which express GST- or 6xhistidine (6xHis)-tagged protein, respectively. 6xHis-KAR and 6xHis-KAR-PRONE were expressed in the *Escherichia coli* strain Arctic Express RP with 0.25 mM IPTG at 12°C. The cells were harvested by centrifugation and lysed in extraction buffer (20 mM Tris-HCl (pH 7.4), 200 mM NaCl, 2 mM $MgCl_2$, 5 mM 2-mercaptoethanol, 1 mM phenylmethane sulfonyl fluoride or phenylmethylsulfonyl fluoride (PMSF), 2 µg/ml leupeptin, 250 µg/ml lysozyme, and 0.2% $C_{12}E_{10}$) with sonication. The bacterial lysate was centrifuged at 100,000 x g for 1 hr. His-tagged protein was captured from the supernatant using nickel-NTA agarose, washed with wash buffer (20 mM Tris-HCl (pH 7.4), 500 mM NaCl, 5 mM 2-mercaptoethanol, 1 mM PMSF, 2 µg/ml leupeptin, and 20 mM imidazole) and eluted with elution buffer (20 mM Tris-HCl (pH 7.4), 150 mM NaCl, 5 mM 2-mercaptoethanol, 1 mM PMSF, and 20% glycerol) with 250 mM imidazole. The eluted proteins were dialyzed against elution buffer and frozen at –80°C.

Bacterial cells expressing GST or GST-MpRop were lysed in extraction buffer (50 mM Tris-HCl (pH 7.4), 150 mM NaCl, 2 mM $MgCl_2$, 1 mM EDTA, 5 mM 2-mercaptoethanol, 1 mM PMSF, 2 µg/ml leupeptin, 100 µM GDP, 250 µg/ml lysozyme, and 0.2% $C_{12}E_{10}$) with sonication. The bacterial lysate was centrifuged at 100,000 x g for 1 hr. GST-tagged proteins were captured from the supernatant using glutathione-agarose, washed with wash buffer I (50 mM Tris-HCl (pH 7.4), 100 mM NaCl, 1 mM EDTA, 5 mM 2-mercaptoethanol, 40 µM GDP, 2 mM $MgCl_2$, 1 mM PMSF, and 2 mµ/ml leupeptin), wash Buffer II (50 mM Tris-HCl (pH 7.4), 500 mM NaCl, 40 µM GDP, 2 mM $MgCl_2$, 1 mM EDTA, 5 mM 2-mercaptoethanol, 1 mM PMSF, and 2 µg/ml leupeptin), then wash buffer I again. GST-tagged proteins were eluted with elution buffer (100 mM Tris-HCl (pH 8.8), 200 mM NaCl, 40 µM GDP, 2 mM $MgCl_2$,10 mM 2-mercaptoethanol, 1mM EDTA, 1 mM PMSF, and 20% glycerol) with 20 mM glutathione. The eluted proteins were dialyzed against elution buffer without GDP and frozen at –80°C.

***In vitro* pull-down assay**

One µg of 6xHis-KAR was incubated with 10 µg of GST or GST-MpROP in Nucleotide

564 Binding Buffer (20 mM HEPES-NaOH (pH 7.4), 5 mM $MgCl_2$, 1 mM dithiothreitol, 0.1%
565 Triton X-100, and 1 mM EDTA) preloaded with 10 μM GDP, GTPγS, or no nucleotide for
566 4 hours at 4°C. The samples were centrifuged with a table-top centrifuge at full speed for 1
567 min, and the supernatant was incubated with Glutathione-agarose resin for 30 min at 4°C.
568 The resins were then washed for three times with Nucleotide Binding Buffer with the
569 respective nucleotide. The resins were then boiled with SDS loading buffer and separated
570 by sodium dodecyl sulfate polyacrylamide gel electrophoresis (SDS-PAGE). The
571 6xHis-tagged proteins were detected by western blot with a mouse anti-6xHis antibody
572 (Santa Cruz Biotech) as the primary antibody, an HRP-conjugated anti-mouse IgG antibody
573 was used as the secondary antibody. GST and GST-MpRop were detected by Coomassie
574 Brilliant Blue staining.
575
576 **GTPγS binding on MpRop**
577 The GEF enzymatic activity of KAR or KAR-PRONE toward MpRop was analyzed using
578 radio-labelled [^{35}S]-GTPγS, as described in previous studies with slight modifications [26,
579 41]. For [^{35}S]-GTPγS binding, 2 μM GST-MpRop in reaction buffer (50 mM Tris-HCl (pH
580 7.4), 1 mM EDTA, 1 mM DTT, and 5 mM $MgCl_2$) was mixed with an equal volume of
581 reaction buffer containing 5 μM [^{35}S]-GTPγS to start the exchange reaction on ice. At given
582 time points, 50 μl aliquots were removed and placed into 450 μl of ice-cold wash buffer
583 (20 mM Tris-HCl (pH 7.4), 100 mM NaCl, and 25 mM $MgCl_2$) with 0.1 mM GTP, then
584 applied to a nitrocellulose membrane filter. The filter was washed three times with 2 to 3
585 ml of ice-cold wash buffer. The amount of [^{35}S]-GTPγS was measured by scintillation
586 counting.
587
588 **RT-qPCR**
589 Total RNA was isolated from the 1-week-old thalli, and mature gemmae, gemma cups, and
590 midribs of 3-week-old thalli of Tak-1 (Fig. 4C) and 1-week-old thalli of the *kar^{KO}#2* line
591 transformed with *proKAR:Citrine-KAR* or *proKAR:Citrine-PRONE* (Fig. 3D) using the
592 RNeasy Plant mini kit (Qiagen). One μg of total RNA was reverse-transcribed in a 20 μl
593 reaction mixture using ReverTra Ace qPCR RT Master Mix with gDNA remover

(TOYOBO). After the reaction, the mixture was diluted with 40 µl of distilled water and 2 µl aliquots were used for quantitative PCR (qPCR) analysis. qPCR was performed with the Light Cycler 96 (Roche) using KOD SYBR qRT-PCR Mix (TOYOBO) according to the manufacturer's protocol. The primers used in these experiments are listed in Table S1. Transcript levels of Mp*EF1a* or Mp*APT* were used as a reference for normalization [42]. RT-qPCR experiments were performed using three biological replicates and technically duplicated.

Phylogenetic Analysis of KAR

For phylogenetic analysis of KAR and RopGEFs, peptide sequences were collected from genomic information of *M. polymorpha* in MalpolBase (http://marchantia.info/), *A. thaliana* in TAIR (http://www.arabidopsis.org), *Physcomitrella patens* [43] and *Selaginella moellendorffii* [44] in Phytozome (https://phytozome.jgi.doe.gov/pv/portal.html), and *Klebsormidium nitens* NIES-2285 in (http://www.plantmorphogenesis.bio.titech.ac.jp/~algae_genome_project/klebsormidium/kf_download.htm) [45]. A multiple alignment of amino acid sequences of KAR and its homologous RopGEFs was first constructed using the MUSCLE program [46] implemented in MEGA6.06 [47] with default parameters, which was performed using a Maximum Likelihood method by PhyML [48] with the LG+G+I substitution model. One thousand bootstrap replicates were performed in each analysis to obtain the confidence support.

REFERENCES

1. Shimamura, M. (2016). *Marchantia polymorpha*: Taxonomy, phylogeny and morphology of a model system. Plant Cell Physiol. *57*, 230-256.
2. Barnes, C.R., and Land, W.J.G. (1908). Bryological papers. II. The origin of the cupule of Marchantia. Bot. Gaz. *46*, 401-409.
3. Proust, H., Honkanen, S., Jones, Victor A.S., Morieri, G., Prescott, H., Kelly, S., Ishizaki, K., Kohchi, T., and Dolan, L. (2016). RSL class I genes controlled the development of epidermal structures in the common ancestor of land plants. Curr. Biol. *26*, 93-99.
4. Steward, F.C., Mapes, M.O., and Mears, K. (1958). Growth and organized development of cultured cells. II. Organization in cultures grown from freely suspended cells. Am. J. Bot. *45*, 705-708.
5. Steward, F.C., Mapes, M.O., Kent, A.E., and Holsten, R.D. (1964). Growth and development of cultured plant cells. Science *143*, 20-27.
6. Steeves, T.A., and Sussex, I.M. (1989). Patterns in plant development, 2 Edition, (Cambridge: Cambridge University Press).
7. Davis, F.T., Geneve, R.L., Wilson, S.E., Hartmann, H.T., Kester, D.E. (2017). Hartmann & Kester's Plant Propagation: Principles and Practices, (Pearson).
8. Hofmeister, W.F.B. (1862). On the germination, development, and fructification of the higher Cryptogamia, and on the fructification of the Coniferae., (London, Pub. for the Ray society).
9. Bowman, J.L., Kohchi, T., Yamato, K.T., Jenkins, J., Shu, S., Ishizaki, K., Yamaoka, S., Nishihama, R., Nakamura, Y., Berger, F., et al. (2017). Insights into land plant evolution garnered from the *Marchantia polymorpha* genome. Cell *171*, 287-304 e215.
10. Ishizaki, K., Chiyoda, S., Yamato, K.T., and Kohchi, T. (2008). *Agrobacterium*-mediated transformation of the haploid liverwort *Marchantia polymorpha* L., an emerging model for plant biology. Plant Cell Physiol. *49*, 1084-1091.
11. Ishizaki, K., Johzuka-Hisatomi, Y., Ishida, S., Iida, S., and Kohchi, T. (2013). Homologous recombination-mediated gene targeting in the liverwort *Marchantia polymorpha* L. Sci. Rep. *3*, 1532.
12. Ishizaki, K., Nishihama, R., Yamato, K.T., and Kohchi, T. (2016). Molecular genetic tools and techniques for *Marchantia polymorpha* research. Plant Cell Physiol. *57*, 262-270.
13. Kubota, A., Ishizaki, K., Hosaka, M., and Kohchi, T. (2013). Efficient

Agrobacterium-mediated transformation of the liverwort *Marchantia polymorpha* using regenerating thalli. Biosci. Biotechnol. Biochem. *77*, 167-172.

14. Sugano, S.S., Shirakawa, M., Takagi, J., Matsuda, Y., Shimada, T., Hara-Nishimura, I., and Kohchi, T. (2014). CRISPR/Cas9-mediated targeted mutagenesis in the liverwort *Marchantia polymorpha* L. Plant Cell Physiol. *55*, 475-481.
15. Nishihama, R., Ishida, S., Urawa, H., Kamei, Y., and Kohchi, T. (2016). Conditional gene expression/deletion systems for *Marchantia polymorpha* using its own heat-shock promoter and Cre/loxP-mediated site-specific recombination. Plant Cell Physiol. *57*, 271-280.
16. Flores-Sandoval, E., Dierschke, T., Fisher, T.J., and Bowman, J.L. (2016). Efficient and inducible use of artificial microRNAs in *Marchantia polymorpha*. Plant Cell Physiol. *57*, 281-290.
17. Ishizaki, K., Mizutani, M., Shimamura, M., Masuda, A., Nishihama, R., and Kohchi, T. (2013). Essential role of the E3 ubiquitin ligase NOPPERABO1 in schizogenous intercellular space formation in the liverwort *Marchantia polymorpha*. Plant Cell *25*, 4075-4084.
18. Takenaka, M., Yamaoka, S., Hanajiri, T., Shimizu-Ueda, Y., Yamato, K.T., Fukuzawa, H., and Ohyama, K. (2000). Direct transformation and plant regeneration of the haploid liverwort *Marchantia polymorpha* L. Transgenic Res. *9*, 179-185.
19. Berken, A., Thomas, C., and Wittinghofer, A. (2005). A new family of RhoGEFs activates the Rop molecular switch in plants. Nature *436*, 1176-1180.
20. Zhang, Y., and McCormick, S. (2007). A distinct mechanism regulating a pollen-specific guanine nucleotide exchange factor for the small GTPase Rop in Arabidopsis thaliana. Proc. Natl. Acad. Sci. U. S. A. *104*, 18830-18835.
21. Duan, Q., Kita, D., Li, C., Cheung, A.Y., and Wu, H.M. (2010). FERONIA receptor-like kinase regulates RHO GTPase signaling of root hair development. Proc. Natl. Acad. Sci. U. S. A. *107*, 17821-17826.
22. Kessler, S.A., Shimosato-Asano, H., Keinath, N.F., Wuest, S.E., Ingram, G., Panstruga, R., and Grossniklaus, U. (2010). Conserved molecular components for pollen tube reception and fungal invasion. Science *330*, 968-971.
23. Nibau, C., and Cheung, A.Y. (2011). New insights into the functional roles of CrRLKs in the control of plant cell growth and development. Plant signaling & behavior *6*, 655-659.
24. Oda, Y., and Fukuda, H. (2012). Initiation of cell wall pattern by a Rho- and microtubule-driven symmetry breaking. Science *337*, 1333-1336.
25. Li, Z., Waadt, R., and Schroeder, J.I. (2016). Release of GTP exchange factor

689 mediated down-regulation of abscisic acid signal transduction through
690 ABA-Induced rapid degradation of RopGEFs. PLoS Biol. *14*, e1002461.
691 26. Gu, Y., Li, S., Lord, E.M., and Yang, Z. (2006). Members of a novel class of
692 Arabidopsis Rho guanine nucleotide exchange factors control Rho
693 GTPase-dependent polar growth. Plant Cell *18*, 366-381.
694 27. Basu, D., Le, J., Zakharova, T., Mallery, E.L., and Szymanski, D.B. (2008). A
695 SPIKE1 signaling complex controls actin-dependent cell morphogenesis through
696 the heteromeric WAVE and ARP2/3 complexes. Proc. Natl. Acad. Sci. U. S. A. *105*,
697 4044-4049.
698 28. Zhang, C., Kotchoni, S.O., Samuels, A.L., and Szymanski, D.B. (2010). SPIKE1
699 signals originate from and assemble specialized domains of the endoplasmic
700 reticulum. Curr. Biol. *20*, 2144-2149.
701 29. Meller, N., Merlot, S., and Guda, C. (2005). CZH proteins: a new family of
702 Rho-GEFs. J. Cell Sci. *118*, 4937-4946.
703 30. Chang, F., Gu, Y., Ma, H., and Yang, Z. (2013). AtPRK2 promotes ROP1 activation
704 via RopGEFs in the control of polarized pollen tube growth. Molecular plant *6*,
705 1187-1201.
706 31. Fu, Y., Gu, Y., Zheng, Z., Wasteneys, G., and Yang, Z. (2005). *Arabidopsis*
707 interdigitating cell growth requires two antagonistic pathways with opposing action
708 on cell morphogenesis. Cell *120*, 687-700.
709 32. Gu, Y., Fu, Y., Dowd, P., Li, S., Vernoud, V., Gilroy, S., and Yang, Z. (2005). A Rho
710 family GTPase controls actin dynamics and tip growth via two counteracting
711 downstream pathways in pollen tubes. J. Cell Biol. *169*, 127-138.
712 33. Etienne-Manneville, S. (2004). Cdc42--the centre of polarity. J. Cell Sci. *117*,
713 1291-1300.
714 34. Park, H.O., and Bi, E. (2007). Central roles of small GTPases in the development of
715 cell polarity in yeast and beyond. Microbiol. Mol. Biol. Rev. *71*, 48-96.
716 35. Humphries, J.A., Vejlupkova, Z., Luo, A., Meeley, R.B., Sylvester, A.W., Fowler,
717 J.E., and Smith, L.G. (2011). ROP GTPases act with the receptor-like protein PAN1
718 to polarize asymmetric cell division in maize. Plant Cell *23*, 2273-2284.
719 36. Facette, M.R., Park, Y., Sutimantanapi, D., Luo, A., Cartwright, H.N., Yang, B.,
720 Bennett, E.J., Sylvester, A.W., and Smith, L.G. (2015). The SCAR/WAVE complex
721 polarizes PAN receptors and promotes division asymmetry in maize. Nature Plants
722 *1*, 14024.
723 37. Gamborg, O.L., Miller, R.A., and Ojima, K. (1968). Nutrient requirements of
724 suspension cultures of soybean root cells. Exp. Cell Res. *50*, 151-158.
725 38. Langmead, B., and Salzberg, S.L. (2012). Fast gapped-read alignment with Bowtie

2. Nat. Methods *9*.

39. Robinson, J.T., Thorvaldsdottir, H., Winckler, W., Guttman, M., Lander, E.S., Getz, G., and Mesirov, J.P. (2011). Integrative genomics viewer. Nat. Biotechnol. *29*, 24-26.

40. Ishizaki, K., Nishihama, R., Ueda, M., Inoue, K., Ishida, S., Nishimura, Y., Shikanai, T., and Kohchi, T. (2015). Development of Gateway binary vector series with four different selection markers for the liverwort *Marchantia polymorpha*. PLoS One *10*, e0138876.

41. Urano, D., Jones, J.C., Wang, H., Matthews, M., Bradford, W., Bennetzen, J.L., and Jones, A.M. (2012). G protein activation without a GEF in the plant kingdom. PLoS Genet. *8*, e1002756.

42. Saint-Marcoux, D., Proust, H., Dolan, L., and Langdale, J.A. (2015). Identification of Reference Genes for Real-Time Quantitative PCR Experiments in the Liverwort Marchantia polymorpha. PLoS One *10*, e0118678.

43. Rensing, S.A., Lang, D., Zimmer, A.D., Terry, A., Salamov, A., Shapiro, H., Nishiyama, T., Perroud, P.F., Lindquist, E.A., Kamisugi, Y., et al. (2008). The Physcomitrella genome reveals evolutionary insights into the conquest of land by plants. Science *319*, 64-69.

44. Banks, J.A., Nishiyama, T., Hasebe, M., Bowman, J.L., Gribskov, M., dePamphilis, C., Albert, V.A., Aono, N., Aoyama, T., Ambrose, B.A., et al. (2011). The Selaginella genome identifies genetic changes associated with the evolution of vascular plants. Science *332*, 960-963.

45. Hori, K., Maruyama, F., Fujisawa, T., Togashi, T., Yamamoto, N., Seo, M., Sato, S., Yamada, T., Mori, H., Tajima, N., et al. (2014). *Klebsormidium flaccidum* genome reveals primary factors for plant terrestrial adaptation. Nat Commun *5*, 3978.

46. Edgar, R.C. (2004). MUSCLE: multiple sequence alignment with high accuracy and high throughput. Nucleic Acids Res. *32*, 1792-1797.

47. Tamura, K., Stecher, G., Peterson, D., Filipski, A., and Kumar, S. (2013). MEGA6: Molecular Evolutionary Genetics Analysis version 6.0. Mol. Biol. Evol. *30*, 2725-2729.

48. Guindon, S., Dufayard, J.F., Lefort, V., Anisimova, M., Hordijk, W., and Gascuel, O. (2010). New algorithms and methods to estimate maximum-likelihood phylogenies: assessing the performance of PhyML 3.0. Syst. Biol. *59*, 307-321.

Figure1-4

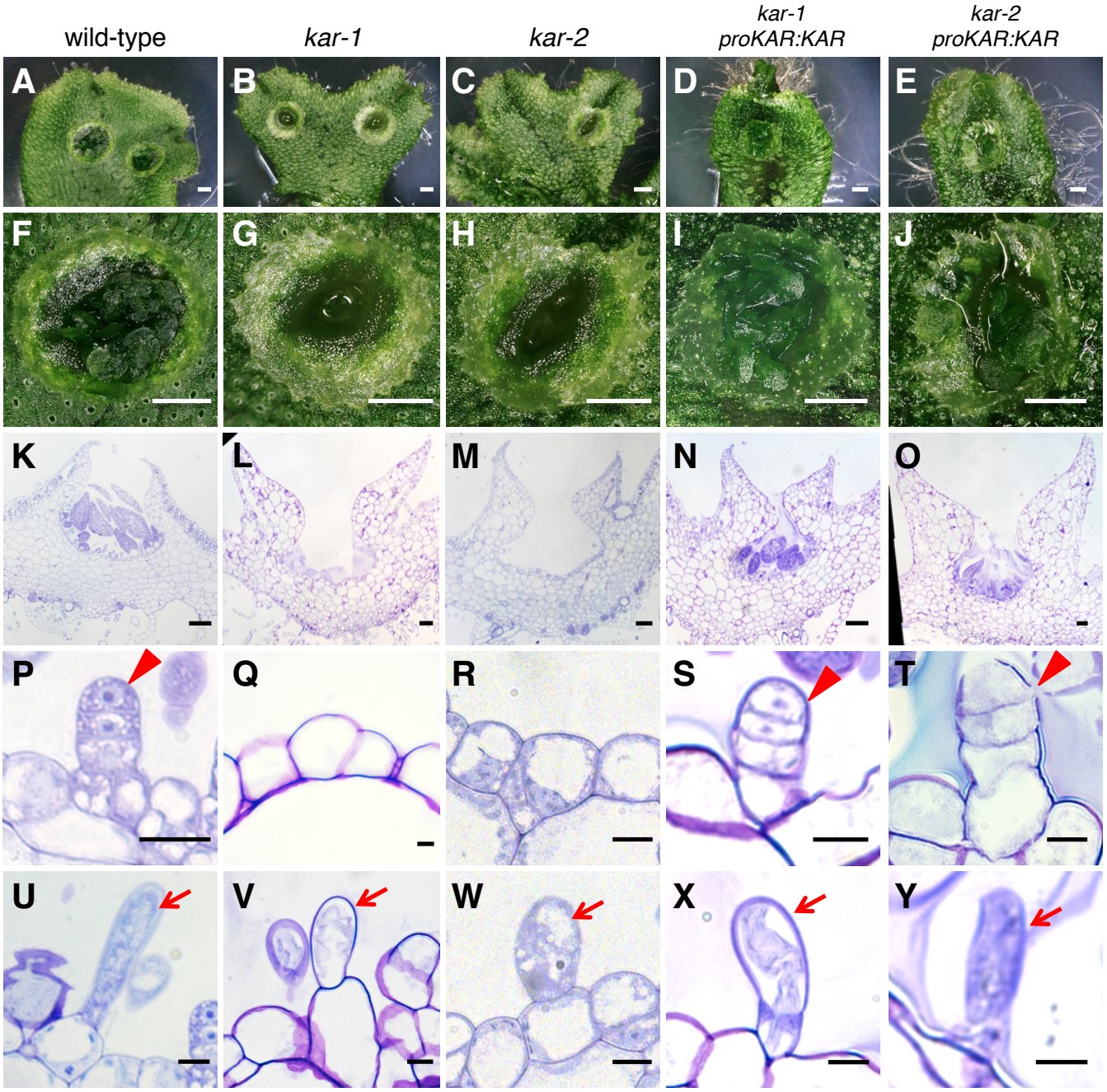

Figure 1. Phenotype of the *kar* mutants and their complimented lines

(A–Y) Five genotypes are presented, one in each column: (first column) wild type, (second column) *kar-1*, (third column) *kar-2*, (fourth column) *kar-1* complementation line (*kar-1* transformed with *proKAR:KAR*), (fifth column) *kar-2* complementation line (*kar-2* transformed with *proKAR:KAR*). **(A–E)** Top view of 2-week-old thalli grown from tips of thalli. Scale bars represent 1 mm. **(F–J)** Surface view of gemma cups in 2-week-old thalli. Scale bars represent 1 mm. **(K–O)** Toluidine-blue-stained transverse sections of gemma cups in 2-week-old plants. Scale bars represent 100 µm. **(P–Y)** Magnified views of toluidine-blue-stained sections of gemma cups in 2-week-old plants. Arrowheads and arrows indicate gemma initials and mucilage papillae, respectively. Scale bars represent 10 µm.

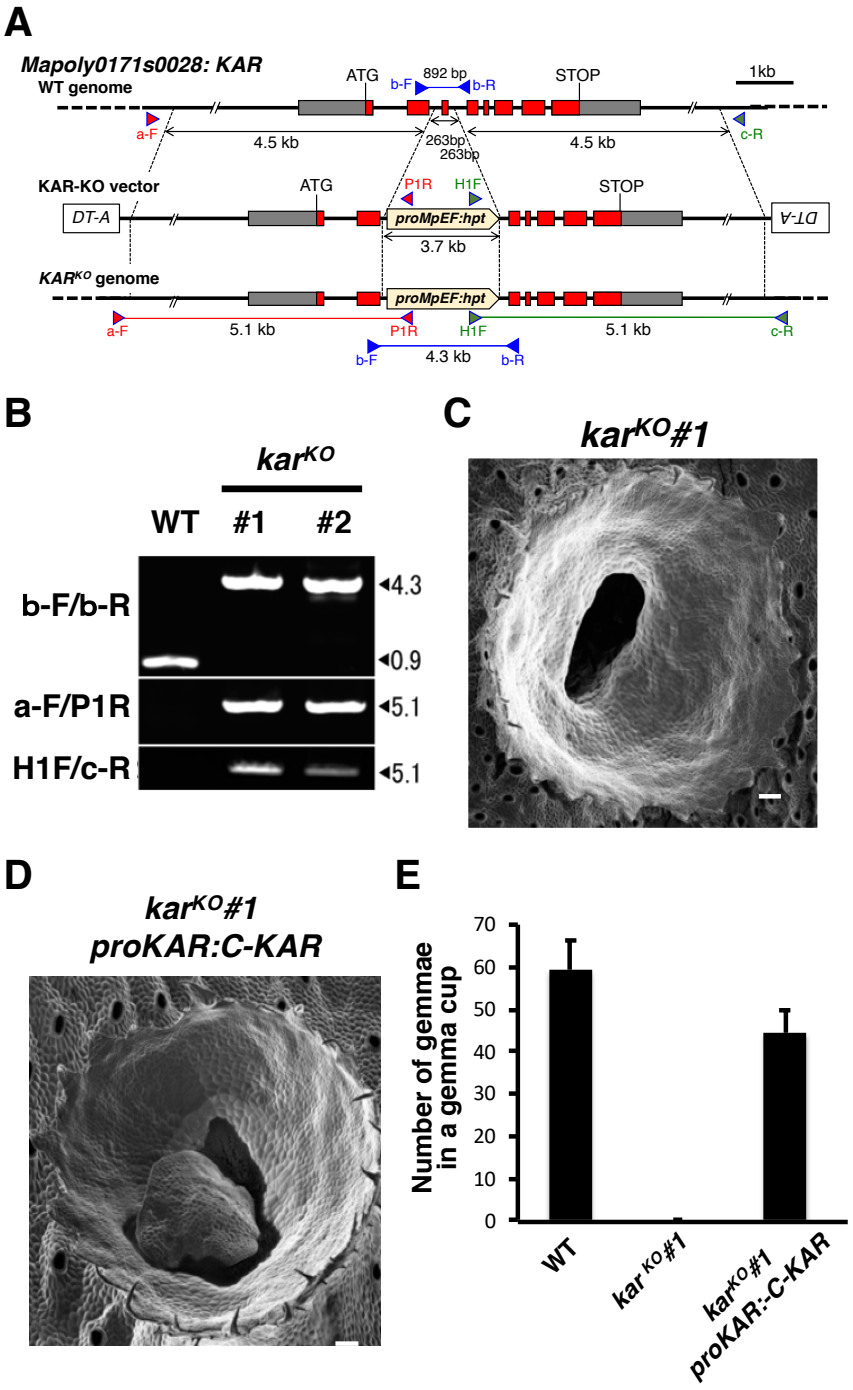

Figure 2. Generation of knockout mutants of *KAR*

(A) Schematic representation of the structure of the wild-type *KAR* locus (top), the construct designed for gene targeting (middle), and the *KAR* locus disrupted in the gene-targeted lines (bottom). Each primer pair used for genotyping is indicated by arrowheads and marked with (F) for forward or (R) for reverse. Open boxes indicate exons. **(B)** Genomic PCR analysis of the KAR^{KO} lines using the primers indicated in (A). **(C, D)** Scanning electron microscopy of gemma cups in three genotypes are presented: kar^{KO}*#1* **(C)**, and a representative kar^{KO} line transformed with *proKAR:C-KAR*, which contains a citrine-fused *KAR* coding sequence under the endogenous *KAR* promoter. **(D)**. Scale bars represent 100 µm. **(E)** Number of gemmae formed in a gemma cup in 3-week-old thalli grown from apical fragments in the wild type, a kar^{KO} line, and a representative kar^{KO} complemented line (Values are means ± SD, n = 5).

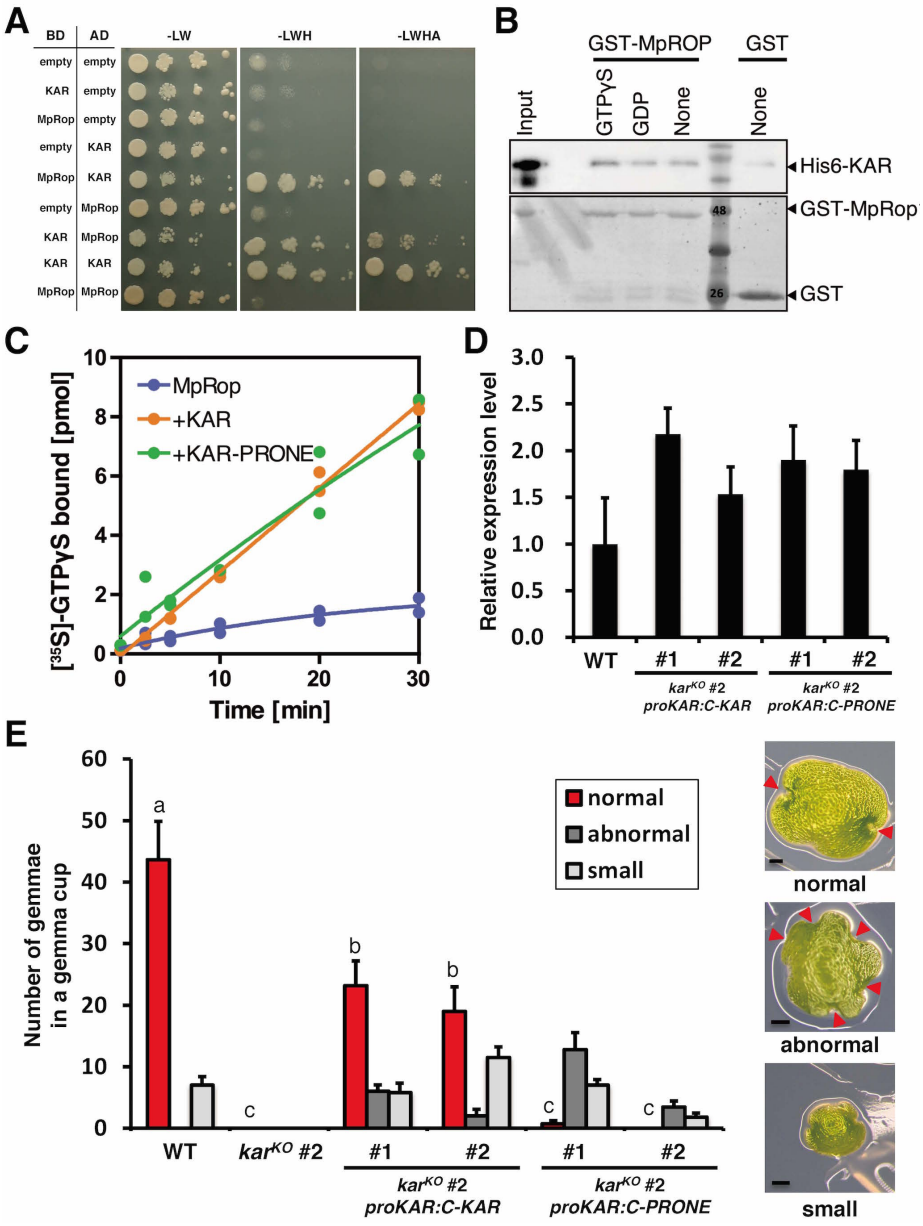

Figure 3. KAR has GEF activity towards MpRop.

(A) Yeast two-hybrid experiments. Clones in the pGBKT7 vector containing the Gal4-binding domain (BD) are noted in the left column and clones in the pGADT7 vector containing the Gal4 activation domain (AD) are noted in the right column. Growth with serial dilutions on the –L, –W dropout media indicates that both pGBKT7 and pGADT7 vectors were present. Growth with serial dilutions on the –L, –W, –H dropout media and –L, –W, –H, –A dropout media indicates a physical interaction between the BD and AD fusion proteins. **(B)** Physical interaction of KAR with MpRop. His6-KAR was pulled down with GST or GST-MpRop1 using glutathione agarose. The pull-down samples were separated on a SDS-PAGE gel, then visualized by western blot with an anti-6xHis antibody. **(C)** GEF activity of the full-length KAR (KAR) or the PRONE domain of KAR (KAR-PRONE) toward MpRop. [^{35}S]-GTPγS binding to 1 µM GST-MpRop1 was analyzed over time at 4° C. Graphs show data from two experiments. Fitting curves were estimated by the one-phase association model in GraphPad Prism software. **(D)** RT-qPCR analysis of *KAR* or *KAR-PRONE* expression in 3-week-old wild type and the respective complementation lines shown in Figure 3E. Mp*APT* was used as a control gene. Data are displayed as means ± SD (n = 3). **(E)** Genetic complementation with the full-length *KAR* and the truncated *KAR* coding sequence containing only the PRONE domain. The histogram shows distribution of the different classes of gemmae in a gemma cup in 3-week-old thalli grown from apical fragments, in WT, a *kar*^{KO} mutant, and two representative *kar* complementation lines with the full-length KAR (*proKAR:C-KAR*) and with the PRONE domain (*proKAR:C-PRONE*) (Values are means ± s.d., n=4~5). Tukey's test was performed for the number of normal gemmae, and letters above the bars indicate significant differences at $p < 0.05$. Right panels show pictures of normal gemma of over 500 µm diameter (normal), abnormal gemma with more than two notches, and small gemma of less than 500 µm diameter.

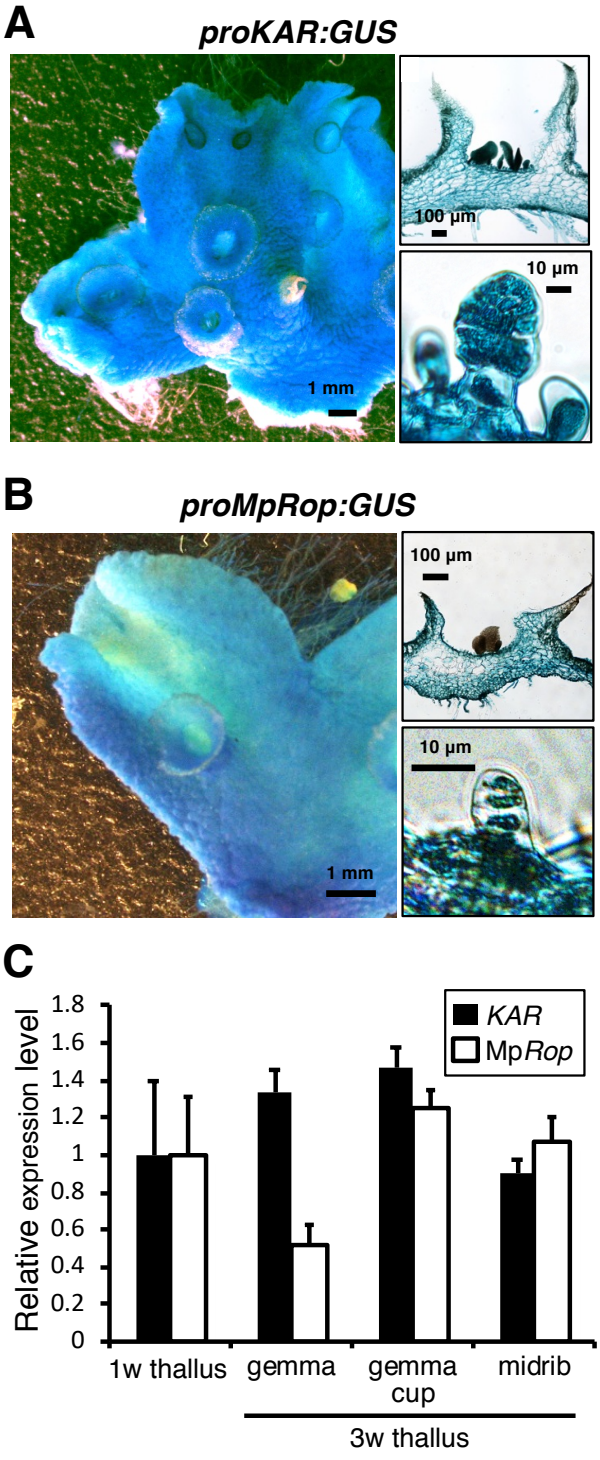

Figure 4. Expression of KAR and MpRop in vegetative tissues

(A, B) Histological GUS activity staining of representative proKAR:GUS **(A)** and proRop:GUS **(B)** transgenic lines. **(C)** RT-qPCR analysis of *KAR* and Mp*Rop* in 1-week-old thalli yet to develop gemma cups (1w thallus), mature gemmae in gemma cups (gemma), gemma cups containing developing gemmae (gemma cups), and midribs. Total RNA was isolated from the respective tissues of Tak-1. *EF1α* was used as a control gene. Data are displayed as means ± SD (n = 3).

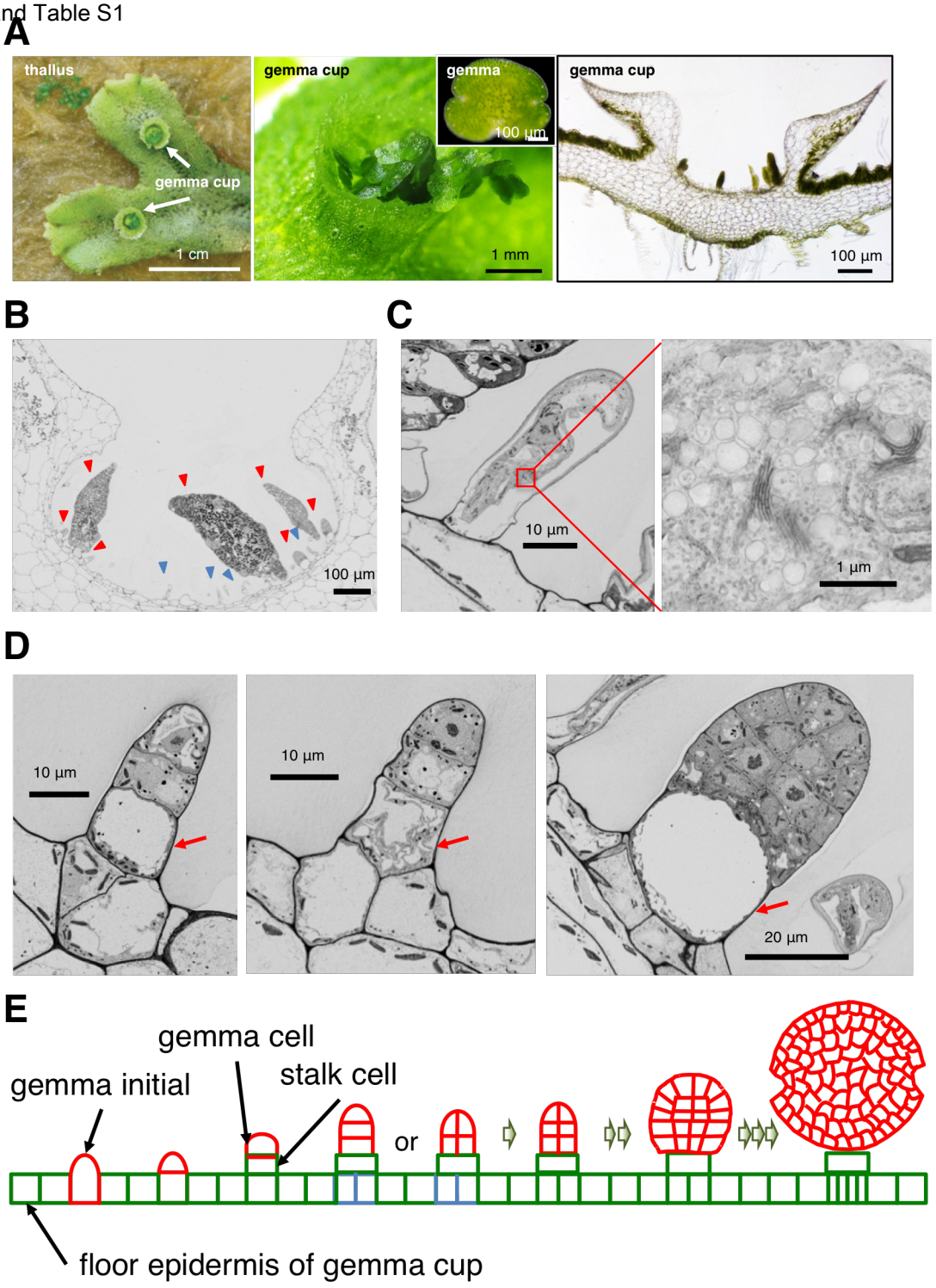

Figure S1. Gemma development in *M. polymorpha*, Related to Figure 1.

(A) Optical observation of gemma and gemma cup in M. polymorpha. Gemma cups formed on the dorsal surface of gametophyte body, thallus. Top view of thallus (left), a close-up view of gemma cup (middle), and a transverse section of a gemma cup (right). (B-D) Electron microscopy in the basal floor of gemma cup. (B) Transverse section of a gemma cup. Red arrow-heads indicate developping gemmae. Blue-arrow heads indicate mucilage papillae. (C) Close up view of mucilage papillae observed at the floor epidermis of gemma cup. The right image shows an enlarged image of indicated cytosolic region in the left image. (D) Close up view of developing gemmae. Red arrows indicate basal stalk cells. (E) Schematic model of gemma development in the floor epidermis of gemma cup.

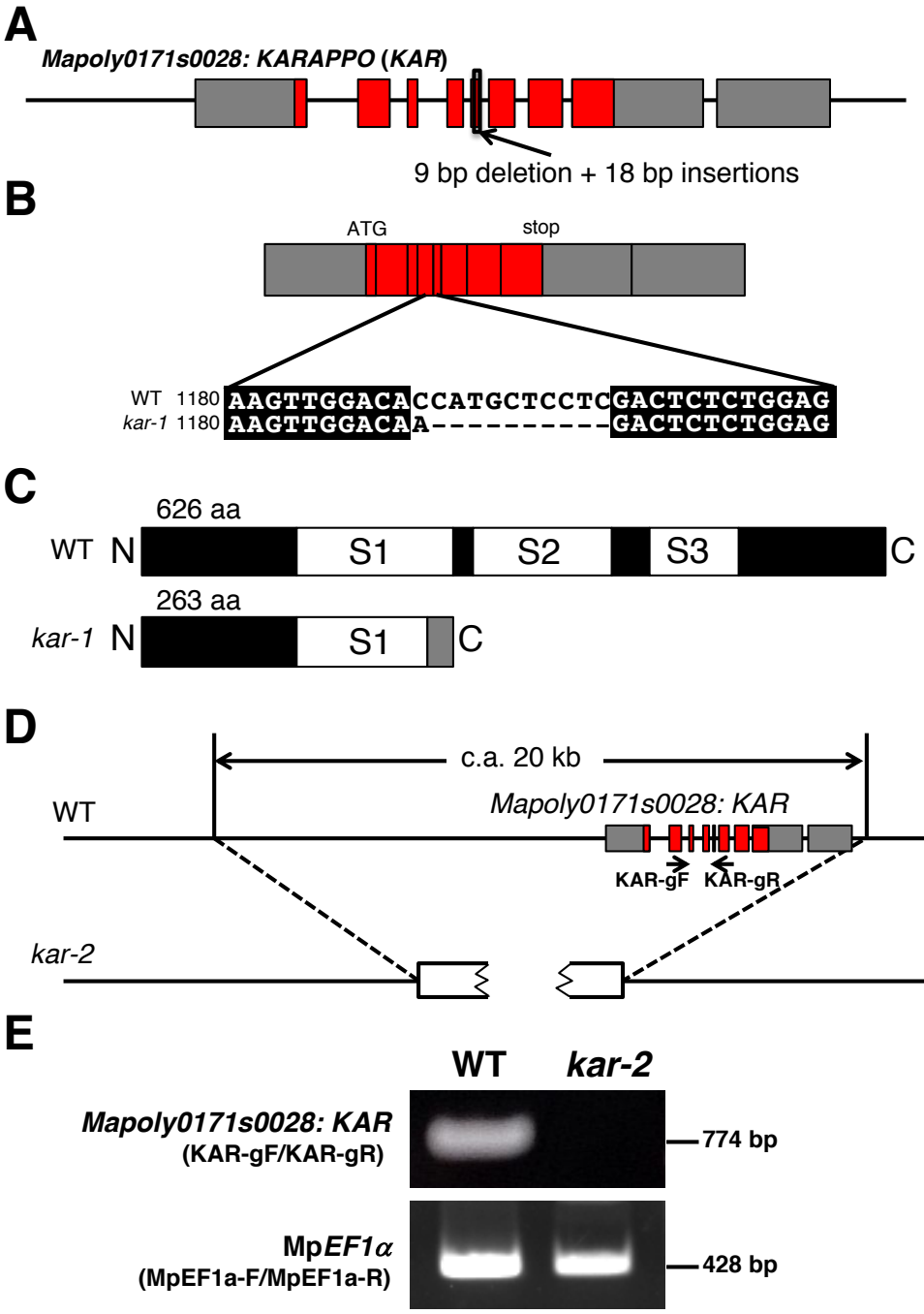

Figure S2. Molecular characterization of *kar-1* and *kar-2*, Related to Figure 1 to 2.
Whole genome analysis revealed respective mutations in Mapoly0171s0028 locus in *kar-1* and *kar-2*. (A) Schematic representation of the Mapoly0178s0028 genomic locus in wild-type and *kar-1*. Gray boxes indicate exons of untranslated region. Red boxes indicate exons of protein coding region. A small deletion found in the *Mapolyo171s0028* locus of *kar-1* genome. (B) cDNA sequences of *Mapolyo171s0028* in *kar-1*. (C) Schematic representation of deduced gene products of *Mapolyo171s0028* in wild-type and *kar-1*. (D) Whole genome analysis revealed c.a. 20 kb deletion in *kar-2*. Broken open boxes indicate partial fragments of pMT plasmid (Takenaka et al. 2000), which was introduced by particle bombardment protocol. A series of genomic PCR suggested that the 5' and 3' region of Mapoly0171s0028 is not adjacent to each other in *kar-2* (data not shown), suggesting occurrence of a genomic rearrangement accompanied with the physical DNA delivery. (E) Genomic PCR of Mapoly0178s0028 in wild-type and *kar-2*. Mp*EFa; M. polymorpha* Elongation Factor alpha gene (Mp*EFa*) was used as a positive control.

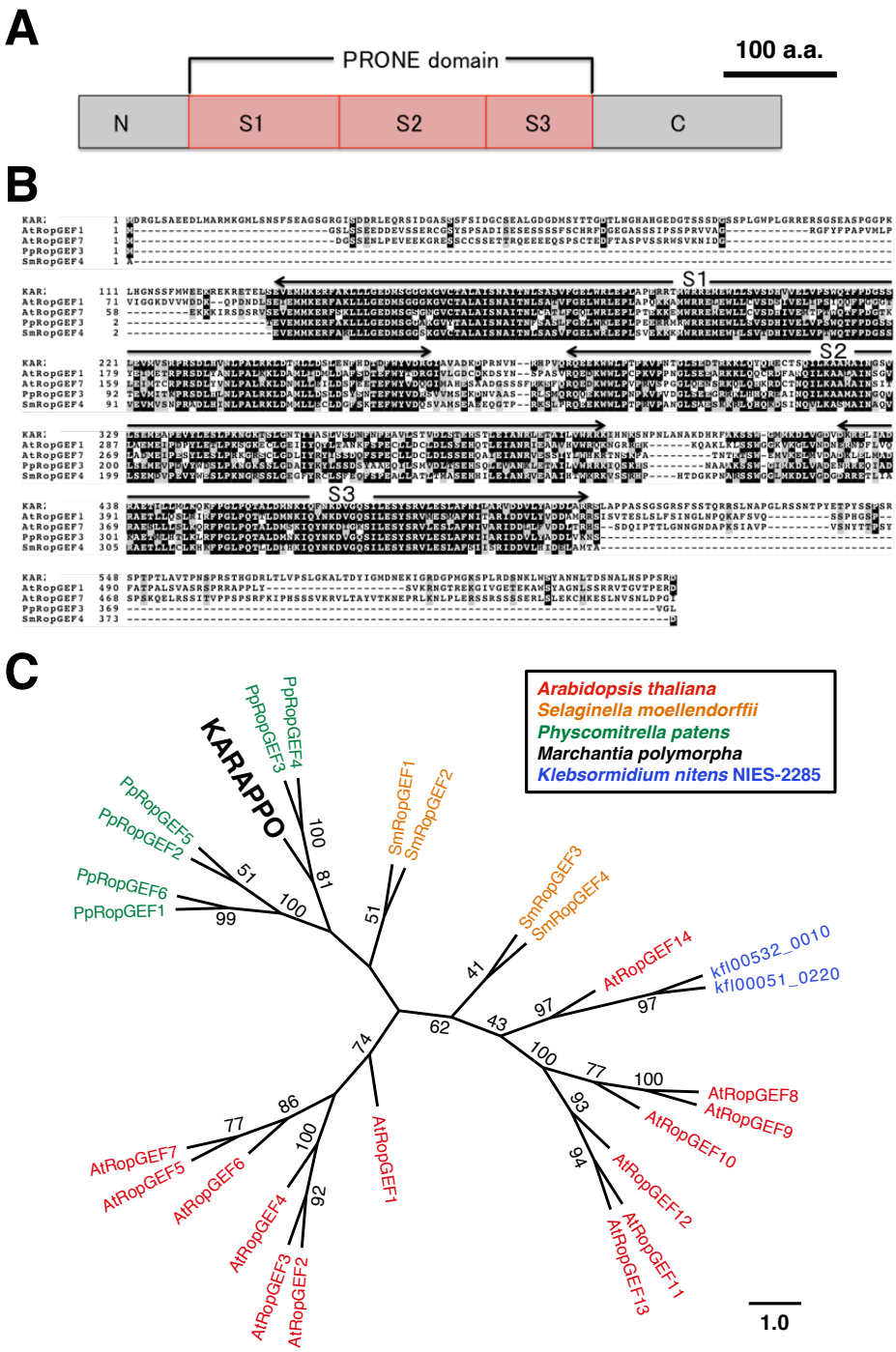

Figure S3. *KAR* encodes a highly conserved PRONE domain of RopGEF, Related to Figure 2 to 3.

(A) A domain structure of the *KAR* gene product. (B) Multiple alignment of the full amino acid sequences of KAR and representative RopGEFs in the moss *Physcomitrella patens*, the lycophyte *Sellaginella moellendorffii* and *Arabidopsis thaliana* RopGEFs. Lines above aligned sequences indicate highly conserved regions in a PRONE domain composed of three subdomains (S1, S2, and S3), which has been in Arabidopsis to be essential for catalytic activity as guanine nucleotide exchange factor of ROP (Gu *et al.,* 2006; Oda *et al.,* 2012). (C) Unrooted Maximum-Likelihood tree of KAR and the other related RopGEF proteins across various plant lineages. The numbers on the branches show bootstrap values calculated from 1000 replicates. The scale bars are evolutionary distance at the ratio of amino acid substitutions.

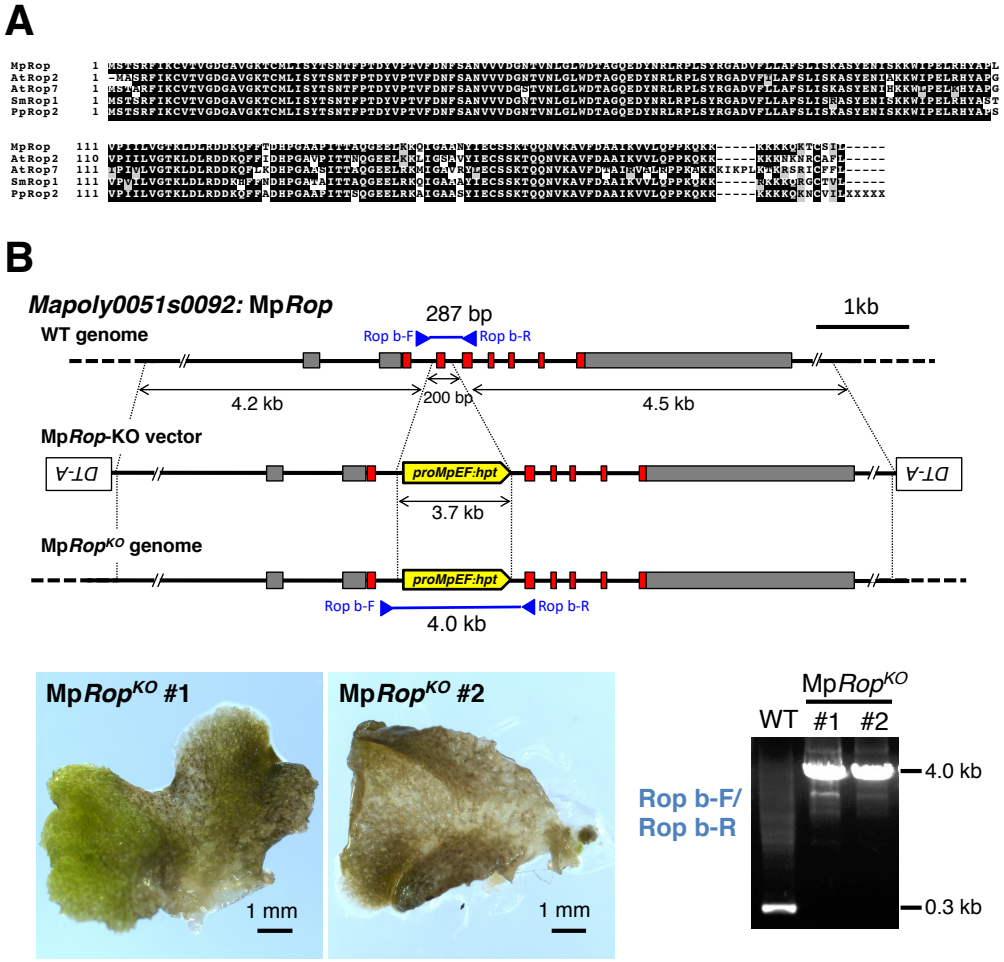

C

	RAC/ROP	RopGEF (KAR)	SPK1	REN	RopGAP	RopGDI	RIC	ICR
Arabidopsis	11	14	1	3	5	3	11	5
Selaginella	2	4	1	1	2	2	1	0
Physcomitrella	4	6	6	2	6	3	1	0
Marchantia	1	1	1	1	1	2	0	0
Klebsormidium	1	2	1	1	1	0	?	0
Chlamydomonas	0	0	0	0	0	0	0	0
Ostreococcus	1	0	1	0	0	0	0	0

Figure S4. RopGTPase and its related gene families in *M. polymorpha*, Related to Figure 4

(A) Multiple alignment of the full-amino acid sequences of MpROP and representative RopGTPases in *P. patens*, *S. moellendorfii*, and *A. thaliana*. (B) Generation of knockout mutants of Mp*Rop*. Schematic representation of the structure of the Mp*Rop* locus in wild type, the construct designed for gene targeting, and the Mp*Rop* locus disrupted in the gene-targeted lines (upper). Phenotype of two independent disruptants of Mp*Rop* gene showed severe impairment of thallus growth, and had died in the early stage of thallus development (lower left). A genotyping of Mp*Rop* indicates successful disruption of the cds structure occurred in Mp*Rop* knockouts (lower right). (C) Relative sizes of Rop signaling gene families in Viridiplantae. Total number of all homologous genes in the indicated gene families are indicated.

Table S1. Oligonucleotide primers used in this study.

Name	Sequence (5'→3')	Usage
kar-1_gF	CCGTATTTGGAGAGTTGTGGA	genomic PCR of *kar-1*
kar-1_gR	ACCGACTGCAGCTTTTGTTT	genomic PCR of *kar-1*
KAR-gF	CGGAAATTCGTCCTTCATGT	genomic PCR of *kar-2* and wild type
KAR-gR	CTCCAGCCTCCACAACTCTC	genomic PCR of kar-2 and wild type
MpEF1a-F	TCACTCTGGGTGTGAAGCAG	genomic PCR of kar-2 and wild type
MpEF1a-R	GCCTCGAGTAAAGCTTCGTG	genomic PCR of kar-2 and wild type
KAR_5IF_F	CTAAGGTAGCGATTAATTAATGAGCTTACCATAATCACCGAGT	Construction of the targeting vector for KAR
KAR_5IF_R	GCCCGGGCAAGGTTAATTAAGGTGGAACATTCTACATCGACAT	Construction of the targeting vector for KAR
KAR_3IF_F	TAAACTAGTGGCGCGCCGACCGGATACGAGTTCTTTTCTT	Construction of the targeting vector for KAR
KAR_3IF_R	TTATCCCTAGGCGCGCCTTGGTAATCTCCAGAACCTCTGA	Construction of the targeting vector for KAR
a-F	TAGACTCGTAGTCCTGGCCCTCAC	For checking of gene targeting site
b-F	GATGGGGACATGAGCTACACCAC	For checking of gene targeting site
b-R	CGAACCAACACGACGTCAGATTA	For checking of gene targeting site
c-R	GTTGTGTGATTGTTGCGGGTAGAG	For checking of gene targeting site
P1R	GAAGGCTTCTGATTGAAGTTTCCTTTTCTG	For checking of gene targeting site
H1F	GTATAATGTATGCTATACGAAGTTATGTTT	For checking of gene targeting site
KARpro_GW_F	GGCCAGTGCCAAGCTTATACAACTGTGGGCTCGACGAAC	Construction of KARpro:KARcds
KARpro_GW_302_R	TGTTGATAACTCTAGATCCATAGCCGAGCCACGTACAG	Construction of KARpro:KARcds
KARpro_GW_305_R	CCATGCTCATTCTAGATCCATAGCCGAGCCACGTACAG	Construction of KARpro:Citrine-KARcds
KAR-cds-F	caccATGGATCGAGGGCTCTCTGCTG	Construction of entry clone containing KAR coding region
KAR-cds-sR	CTAATCACGACTGGGAGGGCTGT	Construction of entry clone containing KAR coding region
PRONE_F	CACCATGGAGGTCGAAATGATGAAGGA	Construction of KAR-PRONE entry clone
PRONE_R	TCAAAGGAACGCCTGGCTAAGTC	Construction of KAR-PRONE entry clone
MpRop_cds_F	CACCATGAGTACTTCCAGGTTTAT	Construction of MpRop entry clone
MpRop_cds_sR	TCACAGGATGGAACATGT	Construction of MpRop entry clone
KAR_WT_Y2H_pGADT7_F	GAGGCCAGTGAATTCatggatcgagggctctctgctg	Constraction of Y2H vector
KAR_WT_Y2H_pGADT7_R	ACCCGGGTGGAATTCctaatcacgactgggagggctgt	Constraction of Y2H vector
KAR_WT_Y2H_pGBKT7_F	ATGGAGGCCGAATTCatggatcgagggctctctgctg	Constraction of Y2H vector
KAR_WT_Y2H_pGBKT7_R	GATCCCCGGGAATTCctaatcacgactgggagggctgt	Constraction of Y2H vector
ROP_WT_Y2H_pGADT7_F	GAGGCCAGTGAATTCatgagtacttccaggtttat	Constraction of Y2H vector
ROP_WT_Y2H_pGADT7_R	ACCCGGGTGGAATTCtcacaggatggaacatgtct	Constraction of Y2H vector
ROP_WT_Y2H_pGBKT7_F	ATGGAGGCCGAATTCatgagtacttccaggtttat	Constraction of Y2H vector
ROP_WT_Y2H_pGBKT7_R	GATCCCCGGGAATTCtcacaggatggaacatgtct	Constraction of Y2H vector
KARpro_F	CACCATACAACTGTGGGCTCGACGAAC	Construction of KARpro:GUS
KARpro_R	ATCCATAGCCGAGCCACGTACAG	Construction of KARpro:GUS
MpRoppro_F	CACCTCCCTCGAGGATTTTTCGAA	Construction of MpRoppro:GUS
MpRoppro_R	AGTACTCATTGTTCACTCCT	Construction of MpRoppro:GUS
PRONEcds_qRT-PCR_F	AAGGAGAGGTTCGCCAAGC	RT-qPCR in Figure 3D
PRONEcds_qRT-PCR_R	TCTACCTCCGAGGGCTTCAA	RT-qPCR in Figure 3D
MpAPT-F	CGAAAGCCCAAGAAGCTACC	RT-qPCR in Figure 3D
MpAPT-R	GTACCCCCGGTTGCAATAAG	RT-qPCR in Figure 3D
KAR-cds-F	CACCATGGATCGAGGGCTCTCTGCTG	RT-qPCR in Figure 4C
KAR-gR	CTCCAGCCTCCACAACTCTC	RT-qPCR in Figure 4C
MpRop_cds_F	CACCATGAGTACTTCCAGGTTTAT	RT-qPCR in Figure 4C
MpRop_cds_sR	TCACAGGATGGAACATGT	RT-qPCR in Figure 4C
MpEF1a-F	TCACTCTGGGTGTGAAGCAG	RT-qPCR control in Figure 4C
MpEF1a-R	GCCTCGAGTAAAGCTTCGTG	RT-qPCR control in Figure 4C
MpRop_5IF_F	ctaaggtagcgattaAGGAGCTGGTTGAAGCCGAC	Construction of the targeting vector for Mp*Rop*
MpRop_5IF_R	gcccgggcaagcttaTCAGTCAACAAGATCAAGGC	Construction of the targeting vector for Mp*Rop*
MpRop_3IF_F	taaactagtggcgcgCACTAATTTTCAATCGTTAT	Construction of the targeting vector for Mp*Rop*
MpRop_3IF_R	ttatccctaggcgcgCACTGATCTTCACTCTCGTC	Construction of the targeting vector for Mp*Rop*
Rop b-F	GCCTCCAGTCGCCGTTCCGG	For checking of gene targeting site
Rop b-R	AGGAAACATCGGATGCCGGG	For checking of gene targeting site